Crawler Design Report

ME112

Team Endangered Beasts and Where to Scoop Them by Newt Salamander
Kathleen Miller, Holly Francis, Heidi Peterson, Kalvin Parker

Mechanical Engineering Design Group
416 Escondido Mall
Stanford University
Stanford, CA 94305-2203

1 Executive Summary

In order to protect the well-being of our salamanders, the design challenge asked for a robot to crawl along an inclined, 13.5cm wide, 9cm high, bumpy, graveled track to retrieve a salamander and guide the rest of the population along the safe path. To meet these design requirements, our team analyzed the theoretical motor capacity, the required torque on the wheels to overcome the bumps, and the ideal gear ratios, and then prototyped and tested several different design types.

Our final design shows these distinctive design choices. The four wheel drive allows the crawler to power over the bumps in the track rather than slipping, with round wheels to enhance efficiency. Despite extra friction, the worm gear transmission allows a gear reduction of 133 to be completed in only two stages. The crawler operates off of 6V to provide enough power to drag the salamander back down the tunnel. Finally, the barbed scoop and wall triggered drop method allowed for a reliable pick up that was still mechanical - unlike other possibilities that we considered such as a grabbing method or using some sort of sticky substance.

We reviewed the efficacy and efficiency of these design choices after test day. The motor has an efficiency of 48.7%, which accounts for loss due to friction and motor resistance. The transmission had an efficiency of 37%. The wheels have an efficiency of 51.3%. The final efficiency of 9.14% allowed the crawler to complete its 1-meter test using 9.7J well under the 40J maximum and even under 10J.

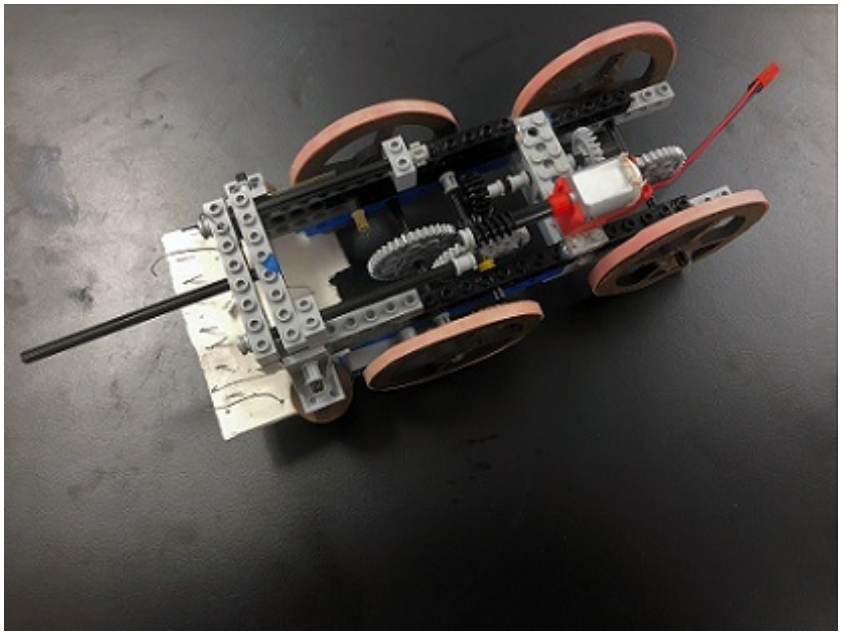

Figure 1.1: *Top view of the final design, featuring the barbed scoop with triggered drop system, round wheels, and the worm gear drive from motor.*

Contents

2 Background

Following an especially rainy season, the plight of the endangered California Tiger Salamander was brought once again into the public eye as the school was forced to contend with protecting these rare amphibians as they crossed from the foothills of the university campus, across Junipero Serra Boulevard, and into the salamander nesting grounds at Lake Lagunita. However, previous efforts to encourage the use of subterranean tunnels have not been as successful as biologists had hoped and ME112 teams were formed to solve the issue of transporting a salamander through the man made tunnel and spreading pheromones to encourage broader use of this tunnel by other salamanders.

Due to size requirements, our crawlers were required to fit inside these tunnels and span no wider than 13.5 centimeters and no taller than 9 centimeters. The crawler was also required to be battery powered which meant minimizing energy use throughout the trip, ideally using fewer than 10 Joules to retrieve and return the salamander. In order to ensure that the salamander would still be able to mate following its journey through the tunnel, any device used had to be able to pickup and transport the salamander without harming it, and all while traversing a gravel covered path with various 0.5 inch bumps.

3 Design Description

The key features of our robotic crawler design are the body, the transmission, and the salamander-retrieving mechanism. Together these aspects of our crawler work together to allow the safe and energy efficient retrieval of the salamander through the tunnel.

3.1 Body Design

The body of the crawler is 9cm wide and 30cm long and, all together with the motor, weighs 183g. With 10cm between the front and rear axles, the salamander retrieval device extends 8cm past the front axle. We chose these dimensions as they allow ample space for our salamander retrieval scoop in front of the wheels, as well as limiting lateral movement while traversing the tunnel.

We chose the distance between the wheels to be 10cm to ensure that the transmission and salamander scoop would fit within the length constraint. Initially, as shown in 3.1 (left), our transmission was too long to allow any added length for the scooping mechanism. Because of this, we decided that, instead of being positioned on side of the transmission, the motor would be placed in a more central portion of the crawler, so as to reduce the number of stages required to transfer the power to both wheels. In 3.1 (right) we ran into the opposite issue, where the wheel size was too large for all four wheels to fit on the drive axles, so we extended the body length to the final design in 3.2.

We chose the width of the body to be 9cm. As shown in 3.1 (left), when our initial body design was equipped with wheels, it extended past the 9.5cm width limit and didn't fit inside the channel. Our next design is shown in 3.1 (right), where the crawler body was markedly thinner. While this allowed us to test the crawler inside the channel, we found that it moved laterally more than anticipated, which would make honing in on a salamander at the other end of the channel difficult. We decided to design the body such that it fit within the 9.5cm channel with wiggle room to spare, but not so much room that it could veer off target. To this end, we also added guide rollers just in front of the front wheels in an effort to keep the crawler aligned through the channel.

3.2 Transmission

The final transmission design is shown in 3.2 and 3.3 and has a gear ratio of 1:133 on the rear wheels (electrical wire side) and 1:111 on the front wheels (scooper side). This difference in gear ratio was actually a design accident that we realized after test day due to confusion between the 20-tooth gear and the 24-tooth gear.This miscalculation resulted in constant wheel slippage, which would have added some to the loss of power. We landed on the ratio of 133 after iterating on theoretical calculations. We also used calculations to determine the gear ratio of our first design, 1:55 and 3V, and during testing we found that our crawler did not have enough torque to drive through the channel. To solve this problem, We increased both the voltage and the gear ratio until the crawler was able to successfully navigate the track.

3.3 Salamander Retrieval Device

Our salamander retrieval device consisted of a barbed ramp and its associated trigger. We decided early on that we wanted to use a ramp style retrieval device, as opposed to a claw or spring loaded trap to capture the salamander and to avoid sticky material to temporarily adhere the salamander on to the crawler, as a mechanical solution to the problem seemed preferable in the challenge description and more repeatable. Early iterations were string activated, similarly to our final design shown in 3.4, but the trigger was not protected from accidental activation and would deploy the ramp at the smallest agitation. To solve this, we developed a hook and pin mechanism that would hold the string, and therefore the ramp, in the up position until ample force had been applied on the protruding shaft. This allowed us to easily traverse the rocky terrain until the crawler made contact with the wall at a specified distance.

The barbed ramp was developed in response to earlier iterations failing to secure the salamander consistently. After noticing that the salamander was able to slide high enough onto the ramp, but would slide off due to lack of friction on the ramp, we iterated on ways to improve ways to "catch" the salamander when it entered the scoop. Our final solution utilized two of the more successful methods to ensure a clean and consistent capture of the salamander: a large, semi-flexible net that was created by layering thin pieces of hooked wire over the ramp, and small, metal barbs that lined the lower surface of the ramp. This net of hooks was used to catch and hold on the larger portions of the salamander, such as the torso and the legs, while the small barbs were intended to prevent smaller parts, such as the claws of the salamander, from slipping.

3.4 Logistics of Salamander Rescue

The straightforward nature of our track meant that the main concerns involved in rescuing the salamander was the consistency of retrieval and the ability to keep the ramp from interfering in the navigation of the course.

After retrieving the salamander, we had to return to the start of the tunnel and prevent the salamander from falling out of the scoop. At this point, the operators were required to reverse leads and bring the crawler back down the tunnel. We used a barbed ramp surface that was hinged at one end to prevent slippage of the salamander and to allow the retrieval mechanism to withstand contact with the ground surface, rather than lifting the scoop back up that would have involved using superfluous mechanisms that would either require more energy or add weight to the final design.

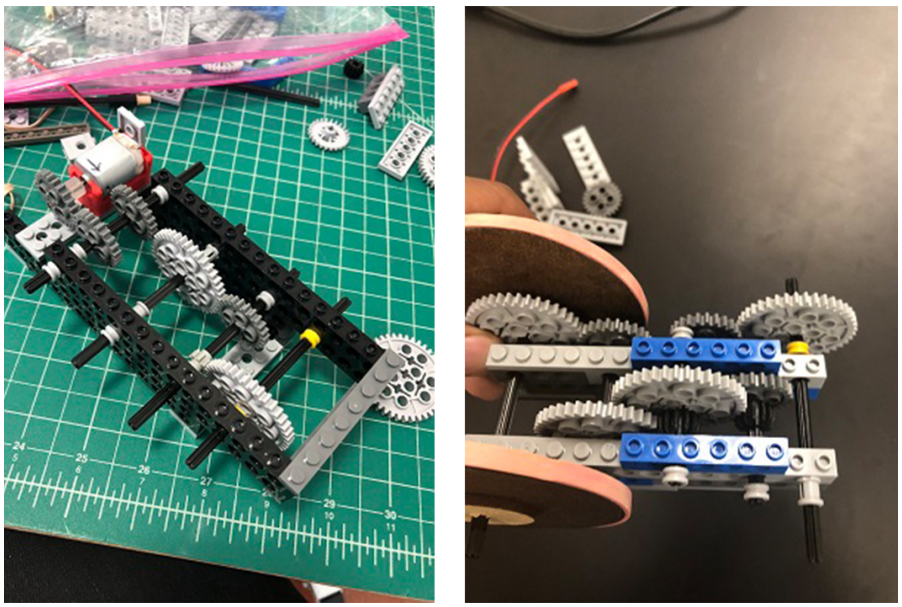

Figure 3.1: *(left) Initial transmission design (right) Later transmission design.*

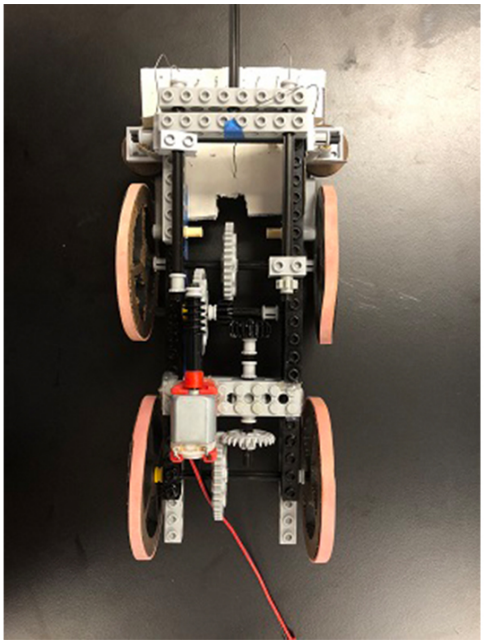

Figure 3.2: *Top view of final crawler design*

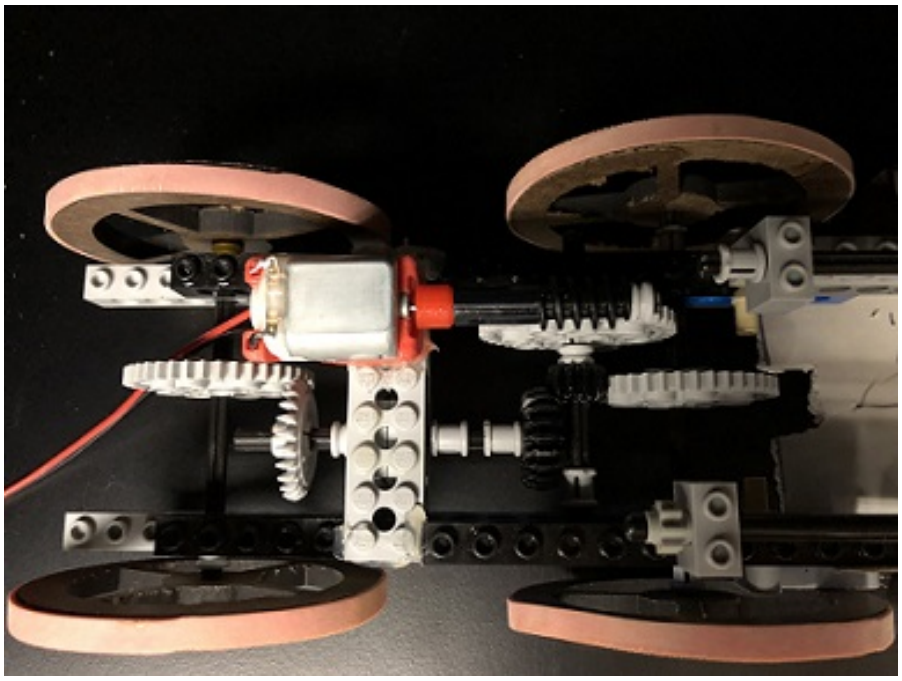

Figure 3.3: *Top view of final transmission design.*

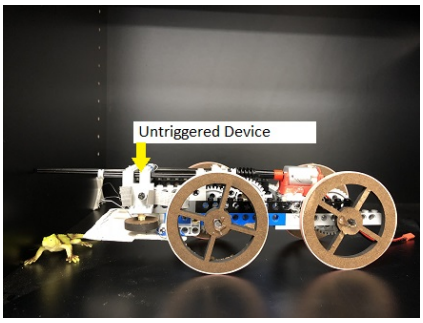

Figure 3.4: *This figure shows the untriggered retrieval mechanism (notice the ramp in the up position.)*

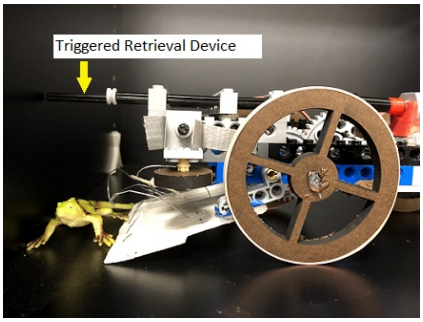

Figure 3.5: *This figure shows the triggered retrieval mechanism as well as the activated ramp.*

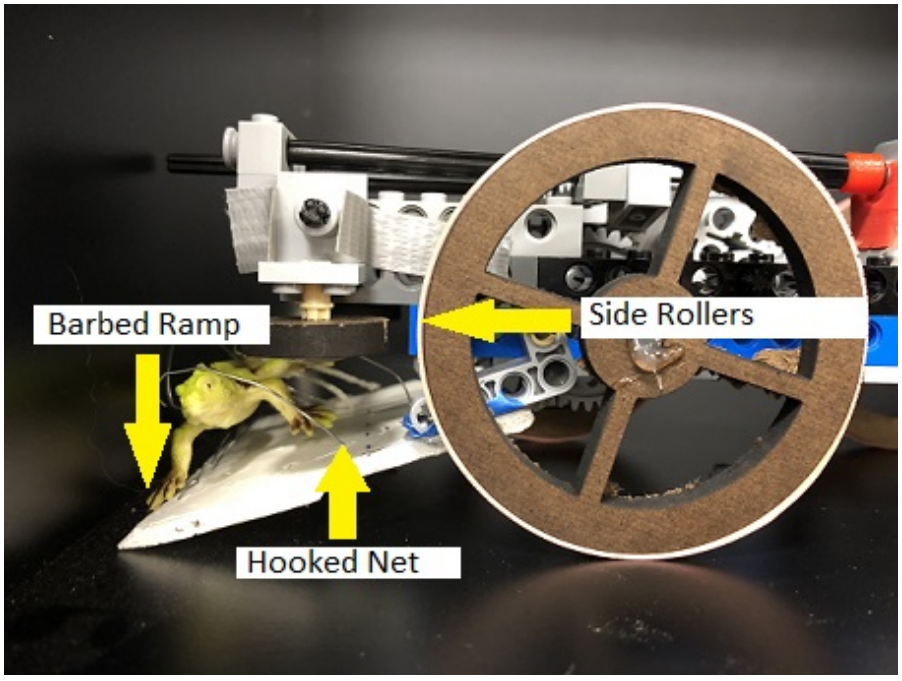

Figure 3.6: *This figure shows the salamander retrieval mechanism, as well as the side rollers used to prevent wall collisions.*

4 Analysis of Performance

Most of the electrical power initially inputted to the crawler from the power source, $P = VI$, was lost to various sources of power loss: motor losses, transmission inefficiency, rolling resistance, and wheel slippage. This resulted in only a small fraction of the initial power ultimately being used to propel the crawler through the channel. Using data from the final test and several additional evaluations, we were able to track our power losses through the crawler and determine the efficiency of each stage: motor, transmission, and wheels. Figure 4.1 is an abstract schematic of each of the sources of power loss in our system. See Table B.2 for index values. Variables for power flow analysis are tabulated in Table **??**.

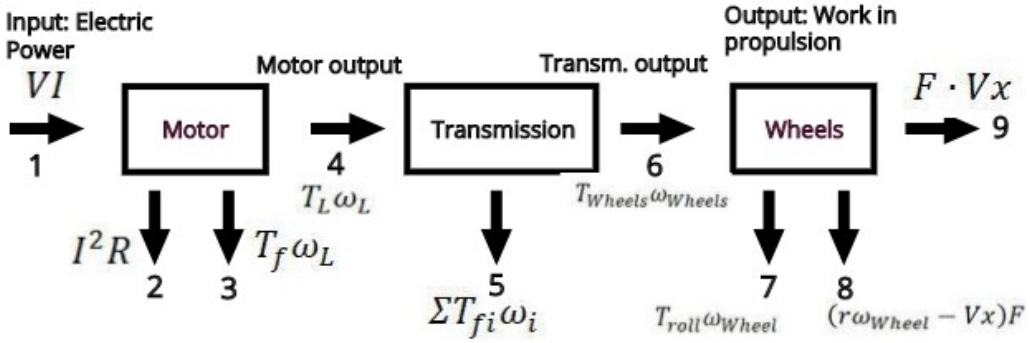

Figure 4.1: *Abstract schematic of power flow for our crawler. Each equation is numbered and referenced is our analysis of the power loss from the initial input of electric power (1) to the final work done by the wheels(9). See Table B.2 for the numerical values of each term.*

4.1 Motor Performance

The first step of our analysis was to characterize the motor and calculate its losses and efficiency. Our motor could be characterized by the following equations, derived from Kirchoff's law and the Lorenz force model:

$$V - IR - k\omega = 0 \tag{4.1}$$

$$kI - T_f = T_L \tag{4.2}$$

where V = voltage, I= current, k = torque constant, T_f = friction torque, T_L = output load torque, and ω = angular velocity in radians/second. We expected there to be two sources of power loss in our motor: power loss due to internal resistance, $P_R = I^2R$, and power loss due to friction, $P_f = T_f\omega_L$, where ω_L = load angular velocity. In order to calculate the magnitude of these losses, we performed stall and no-load tests on the motor and used the experimental

data to calculate the internal resistance R, torque constant k, and friction torque of the motor T_f. With a given V and corresponding I, we would then be able to determine the amount of power being lost to each source.

During the stall test, we drove the motor at varying voltages while holding the shaft so it could not rotate, and measured the stall current, I_s. By setting $\omega = 0$, equation B.1 simplifies to $V = I_s R$, from which we could calculate values of R. We averaged the values of R from each test to find the motor resistance (Table 4.1). During the no-load test, we drove the motor at varying voltages and measured the resulting current and angular velocity. From equation B.1, we calculated values of k, which we averaged to find the motor torque constant (Table 4.1). By setting $T_L = 0$ (allowing the motor to spin freely), equation B.2 simplifies to $T_f = kI_{nl}$, where I_{nl} = no-load current. Using this equation, we can calculate values of T_f, which we again average to find the motor friction torque. Equations are listed and and data from the stall and no-load tests is tabulated in Appendix B.3.

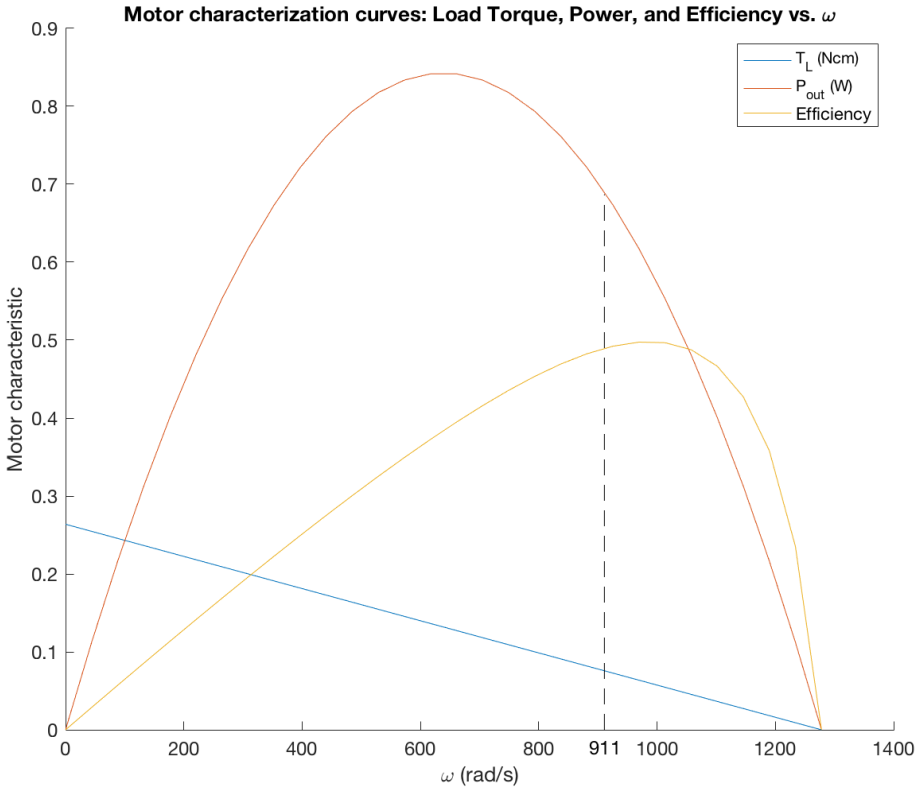

Figure 4.2: *Current, power and efficiency for our electric motor. The dotted line marks where on the plot our crawler was operating.*

Having calculated the motor resistance, torque constant, and friction force, we were able to generate the motor curves to determine the load torque, power output, and efficiency of our motor as functions of angular velocity (Figure B.3). We determined that our motor would run its peak efficiency ($\eta_m = 50\%$) at $\omega_L = 970$ rad/s and peak power ($P_m = 0.84$ W) at $\omega_L = 617$ rad/s. In designing our crawler, we aimed for our motor to run at a speed in between

those two points, and ultimately ran the motor at 911 rad/s (represented in Figure B.3 by the dashed vertical line), which resulted in an output power of 0.69 W and efficiency of 49%.

4.2 Rolling Performance

The next step in evaluating the power flow was determining the power losses due to rolling resistance and slippage, and the efficiency of the wheels stage of our crawler. In our free body diagrams (Figures 4.3, 4.4), we modeled rolling resistance as a force, F_{roll} opposing the direction of movement of our crawler, acting at the center of each wheel. In the case of our crawler, it was difficult to separate F_{roll} from the force used to propel the crawler through the channel, F_{out}, so in the following analysis, we consider $F_{pull} = F_{roll} + F_{out}$. To determine F_{pull}, the amount of force required to pull our crawler (with transmission disconnected) up the channel, we performed the drag test on our crawler. The drag test involved attaching to our crawler a string that went over a low-friction pulley at the end of the channel. With the transmission disconnected, we found the mass, m, required to pull the crawler through the channel at approximately the same speed that it moved in the final test. We then calculated $F_{pull} = mg$, where $g = 9.81$ m/s is the gravitational constant.

A significant source of power loss in the wheels stage of our crawler was slippage. This was especially relevant due to the gravel in the channel and a design flaw in our transmission. After the final test, we discovered that the wheel axles spun at different rates, which meant that the back wheels, which spun at a faster rate than the front wheels, would be slipping more than the front. The power loss due to slippage is represented by $P_s = (r_w\omega_w - v_x)F_{pull}$, where r_w = wheel radius, v_x = translational velocity of the crawler, and ω_w = angular velocity of the wheels. We calculated ω_w by averaging the angular velocities of the front and back axles, $\omega_{w,f} = \frac{\omega_L}{GR_f}$ and $\omega_{w,b} = \frac{\omega_L}{GR_b}$, where GR_f and GR_b are the gear ratios of the front and back wheels, respectively. We calculated the output power of the wheels, P_w, which goes towards propelling the crawler through the channel and overcoming rolling resistance, using the equation, $P_w = F_{pull}v_x$. From here, we determined the power output from the transmission, $P_t = P_w - P_s$, and the efficiency of the wheels, $\eta_w = \frac{P_w}{P_t} = 51\%$. At this point, we were also able to calculate the total efficiency of the crawler, $\eta_{net} = \frac{P_w}{P} = 9\%$. Equations are listed and and data from the drag test is tabulated in Appendix B.4.

4.3 Transmission Performance

The final step in our power flow analysis was to determine the transmission power losses and efficiency. At first, we attempted to perform a pulley test on each output of the transmission (front and back axles), in which we attached drums to the transmission input (where the motor attaches) and output (where the wheels attach). During the test, we lifted a cup of gravel attached to the output drum by attaching another cup of gravel to the input drum. We added gravel to the output cup until it was barely moving upwards, and weighed both cups. For each axle, we computed the theoretical mass that the input cup should have been able to lift assuming 100% efficiency, $m_{th} = m_i GR$, where m_i = mass of input cup and GR = gear ratio. We compared m_{th} to the mass of the output cup, m_o, to find the transmission efficiencies of each axle, $\eta_t = \frac{m_o}{m_{th}}$. We then averaged these values to find the total transmission efficiency, $\eta_t = 16\%$. However, we suspected that this test greatly underestimated the transmission

efficiency due to limitations of the test, such as the need to overcome static friction when lifting the gravel and excessive bending of the Lego parts due to a large m_{th}, which would result in a low m_o. Instead, we decided to back-calculate the transmission efficiency using the equation $\eta_t = \frac{\eta_{net}}{\eta_m \eta_w} = 37\%$. Equations are listed and and data from the pulley test is tabulated in Appendix B.5.

4.4 Performance Summary

The efficiencies and power losses of each stage of the crawler can be found in Table 4.2. Starting with the 9.71 J required to move the crawler up and down the ramp (1 m each way), 4.98 J were lost in the motor stage (3.39 J lost to coil resistance and 1.59 J lost to friction), 2.99 J were lost in the transmission stage, and 0.85 J were lost in the wheels stage due to slippage, leaving 0.89 J to propel the crawler in the channel and overcome rolling resistance. Since our crawler does no work, a strict estimation of our overall efficiency would be 0%. However, if we consider moving the mass of the crawler through the channel and overcoming rolling resistance to be work, then our efficiency would be 9.14%.

4.5 Free Body Diagrams

Drawing Free Body Diagrams allowed us to make a few educated guesses about where to begin our design process. Two diagrams in particular were helpful as we were trying to understand the different forces acting on the crawler. The first (Figure 4.3) was a diagram of the full structure, including the torques on both the front wheels and the back wheels (four wheel drive), the tangential force where the wheels are in contact with the ground, the rolling resistance, gravity as the crawler climbed the slight incline, and the normal force. In this diagram, the crawler is assumed to be traveling at a constant velocity (no acceleration), so sum of the forces acting on the structure balance to zero. Taking a closer look at the directions that the forces and moments are acting, the tangential force on the wheels balances with the rolling resistance and the component of gravity along the incline. The moment caused by this tangential force is balanced by the torque on the wheel axles from the motor. The normal force is balanced by the perpendicular component of the gravitational force.

$$\perp F_g = mgcos(\theta) \tag{4.3}$$

$$\Sigma F\hat{t} = ma\hat{t} = F_t - F_{roll} - mgsin(\theta) \tag{4.4}$$

Force balance when moving at a constant velocity up the incline. This FBD also applies when the crawler is descending down the incline, with the added friction of the captured salamander dragging along the ground.

The second diagram (Figure 4.4) looks more closely at the demands of the track on the motor. This diagram is intended to provide a rough estimate of the torque required on the wheels for the crawler to roll over the given bump height of 0.5 in. In this case, a single wheel is drawn as it is about to lift off of the ground, over the bump. The calculations are performed for the worst case scenario, when the crawler has just enough torque available. In this edge case situation, the crawler can be assumed to be stationary, with the motor at a near

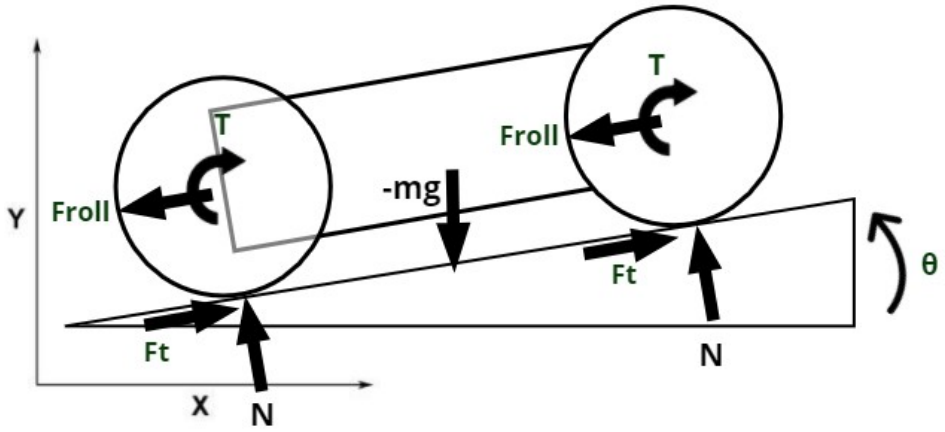

Figure 4.3: *Free body diagram for Crawler moving up inclined gravel*

stall. Analyzing the individual forces, the tangential force of the wheel is balanced with the component of the normal force on the edge of the bump that is in line with the incline, the component of gravity along the incline, and the drive from the back wheels. The geometry of the problem is diagrammed below, with α as the angle between the perpendicular and the line of action of the normal force. This angle can be calculated using trigonometry as shown in the figure.

Note that rolling resistance is not accounted for in the derivation of the required torque; this free body diagram is only intended to give a rough estimate for the gear ratio and the motor power required. The rolling resistance can only be added to the balance through experimental testing, as is done in the final design analysis.

$$\frac{R-h}{R} = cos(\alpha) \tag{4.5}$$

$$\Sigma F\hat{t} = 0 = F_T + F_{4WD} - N_t \tag{4.6}$$

$$0 = \frac{\tau_w}{R}cos(\alpha) + \frac{\tau_w}{R} - \frac{1}{2}mgcos(\theta)tan(\alpha) \tag{4.7}$$

The theoretical torque required is 0.214 lb-in. Using this approximation, we designed our first gear transmission and iterated from that point. This value does not include rolling resistance of the gravel.

4.6 Strength Estimate

The stress on each stage in the gear train was calculated using Lego material constants and given gear ratios and radii. Note that the front wheel drive and the back wheel drive are calculated separately. For a full list of the constants used, see Appendix section C.2. From these approximations, the worst case gear can be assumed to be the 12-tooth gear in the middle of the transmission that drives both shafts. Table 4.1 outlines the stresses calculated for each

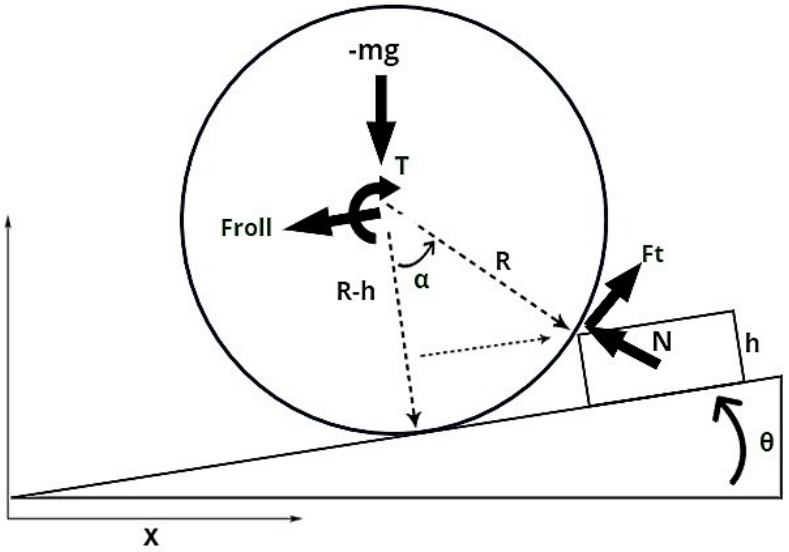

Figure 4.4: *Free body diagram for wheel going over bump at point of stall; used to calculate maximum bump height for a given wheel torque or visa versa.*

gear. This is as expected given that this gear is both the smallest and has two contact points. The stress at this point is 1033.5psi, which is still under the allowable stress 4270psi. See Appendix C for constants and equation used to calculate the allowable stress.

$$\sigma_b = \frac{F_t P}{bJ} K_m K_o K_v; \tag{4.8}$$

The stress on the worm gear was also calculated using Lego material constants and given radii. While the worm gear has an available stress of 212.7psi, equation C.2, the failure is often not on the worm gear itself, but on the teeth of the mating gear. Thus it is important to understand the forces associated with the worm gear and its mating gear. We found the force on the mating gear to be 0.02N, equation C.3. Using this force and the area of the mating gear tooth, the stress imparted to the mating gear from the worm gear is 322psi, which is below the allowable maximum value of 516.8psi.

Of the axial, radial, and tangential forces on the worm gear, we found the axial force to be the largest in magnitude, at 1.17N, equation C.4, which acts in the direction of moving the worm gear down the shaft of the motor. To counteract this force, we used a bushing placed next to the worm gear to keep it in place on the shaft. A detailed analysis of the force calculation is in Appendix section C.

Gear	σ_b (psi)
Worm	212.7
40-tooth	516.8
12-tooth (note two contact points)	1033.5
40-tooth	279.32
20-tooth	344.5
24-tooth	254.1
40-tooth	221.5
Max stress per gear	4270

Table 4.1: *Lifetime stress on each gear.*

5 Redesign for Improved Performance and Reliability

To reapply this design to collect the much larger Tasmania Tiger Salamander, we would need to address a few key issues:

- The scoop is too small and the barbs are not strong enough
- The scoop is too far forward and unbalances the crawler once collecting the larger salamander
- The torque on the wheels is not high enough to manage the extra friction of dragging back the larger salamander

There are a few structural changes to make before addressing the transmission that are essential to handle a larger salamander. The scoop would need to move towards the center of the cart, underneath the gear transmission. This would accomplish fitting the larger salamander, moving the weight distribution towards the center, and allowing the angle of incline of the ramp to be smaller all three of these points would improve the collection system. Moving the center of mass towards the middle of the crawler would also improve all around traction and equalize forces on the two wheel axles. The design change would force us to increase the effective distance of our trigger mechanism to ensure the ramp has proper time to deploy in its new position (a problem in our current design). The transmission design would also need to be altered. In order to create the aforementioned space inside of the transmission, we would begin by pushing all gearing towards the outside of the cart which would allow a full use of interior space of the crawler. The torque required to lift this much larger salamander could be overcome by increasing wheel surface area, increasing the gear ratio, and perhaps using a higher voltage to manage the extra weight. Since the crawler is four wheel drive, we can take advantage of the opportunity to have two different gear ratios and therefore two different wheel sizes on each axle. This would require testing, but perhaps improve ground contact with larger wheels on the front axle, where the more of the salamander's weight will be.

6 Conclusions

In a final performance test, our crawler design was successful on its third run. We struggled initially with grabbing and securing our salamander, but after regrouping and returning to an earlier design, we were able to successful retrieve and transport the salamander. Overall, this third run was more successful as we stayed under our energy use goal of 10 joules and were able to minimizing the switching of leads, which had been our main method of ensuring successful retrieval in testing.

On the more technical aspects of our result, our final design was able to stay close to peak efficiency at 6 volts, drawing an average of .25 amps on our initial journey and .22 amps on our return journey. Wheel slippage was low in our testing, although the difference in gear ratios did leave to some inherent wheel slippage in the design, but this was largely not an issue in the completion of the mission. This characteristic, along with our wheel design along with the rubber bands we used to improve traction were very successful in ensuring a quick and efficient journey for our crawler. We were also able to improve performance by adding on horizontal stabilizers to improve our straight line performance in the tunnel.

With regards to repeatability and consistency, we did initially run into some issues with our barbed ramp system and the effectiveness of the method in a situation where salamander wasn't able to slide onto the scoop, however, after adding additional barbs, the repeatability greatly increased and we weren't limited to only being able to lift the salamander in a set orientation. Our force activated trigger mechanism was also highly successful and the simplicity of the set up, along with the limited number of moving parts, meant that we were able to run multiple test trials quickly, and solve any issues that arose on the spot in our final presentation runs.

A Design Iterations

A.1 Body Design Iterations

In our first crawler iteration, we made an initial guess for approximate wheel rotations per minute and torque required. Using these theoretical values, we were able to calculate the gear ratio of 55 using 3V. From this design we learned to keep track of width. Our approach was to build the transmission and body separately, to allow for multiple project members to work on different parts of the crawler at the same time, however in doing so the width of the crawler was extended beyond what was able to fit within the channel.

In our second crawler iteration, we used a narrower transmission design. After our crawler was so wide in the previous design, we explored how narrow we could go with this design. In the last stage of this transmission we made the mistake of decreasing the gear ratio, giving an overall transmission ratio of 14. In this iteration, in addition to further exploring width, we also learned a lesson in Lego spacing. As we added stage after stage in our transmission, the logistics of geometrically housing everything became very challenging, which led to our gearing mistake in the final stage.

Learning from our second crawler design, our third crawler iteration featured a gear ratio of 5. While the overall robustness of the design was stronger, the gear ratio decreased, which caused us to quickly move on from this design. While trying to make the overall shape of the transmission more durable, the gear placement was less than ideal as again, in the late stages of the transmission, we decreased the gear ratio.

In our fourth and penultimate design, we decided to utilize our worm gear. Having seen low gear ratios in the past two designs, our focus this time was to increase the gear ratio, which we did by achieving a gear ratio of 44. While this result was promising, in the process of increasing the gear ratio this crawler design became two wheel drive. After testing this crawler in the channel, and watching it fail to surmount the gravel barricades, we decided that moving forward we wanted our crawler to be four wheel drive as to reliably traverse the bumpy channel.

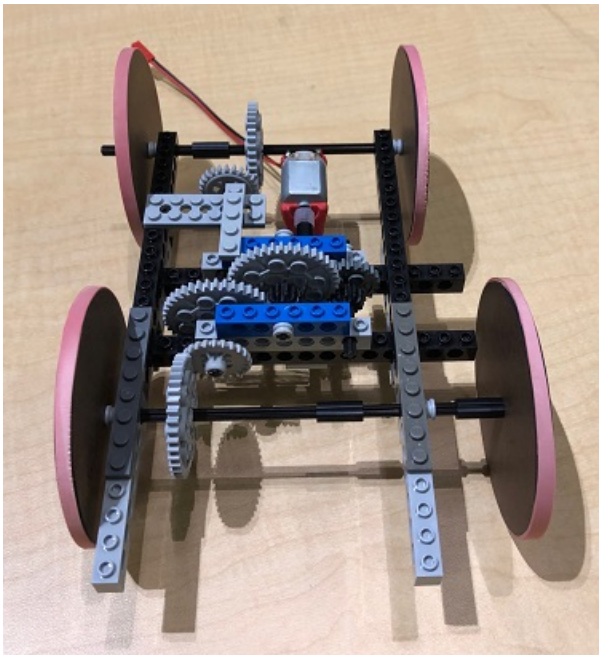

Figure A.1: *Crawler iteration 1.*

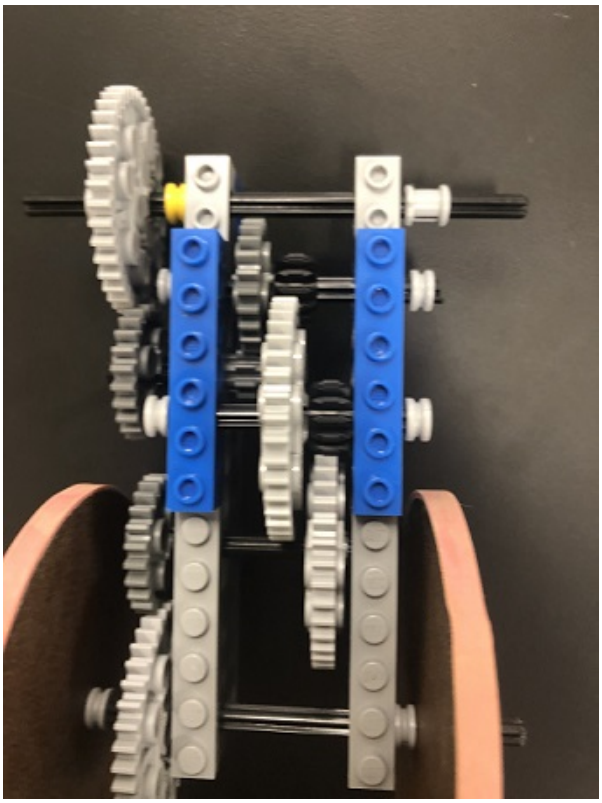

Figure A.2: *Crawler iteration 2.*

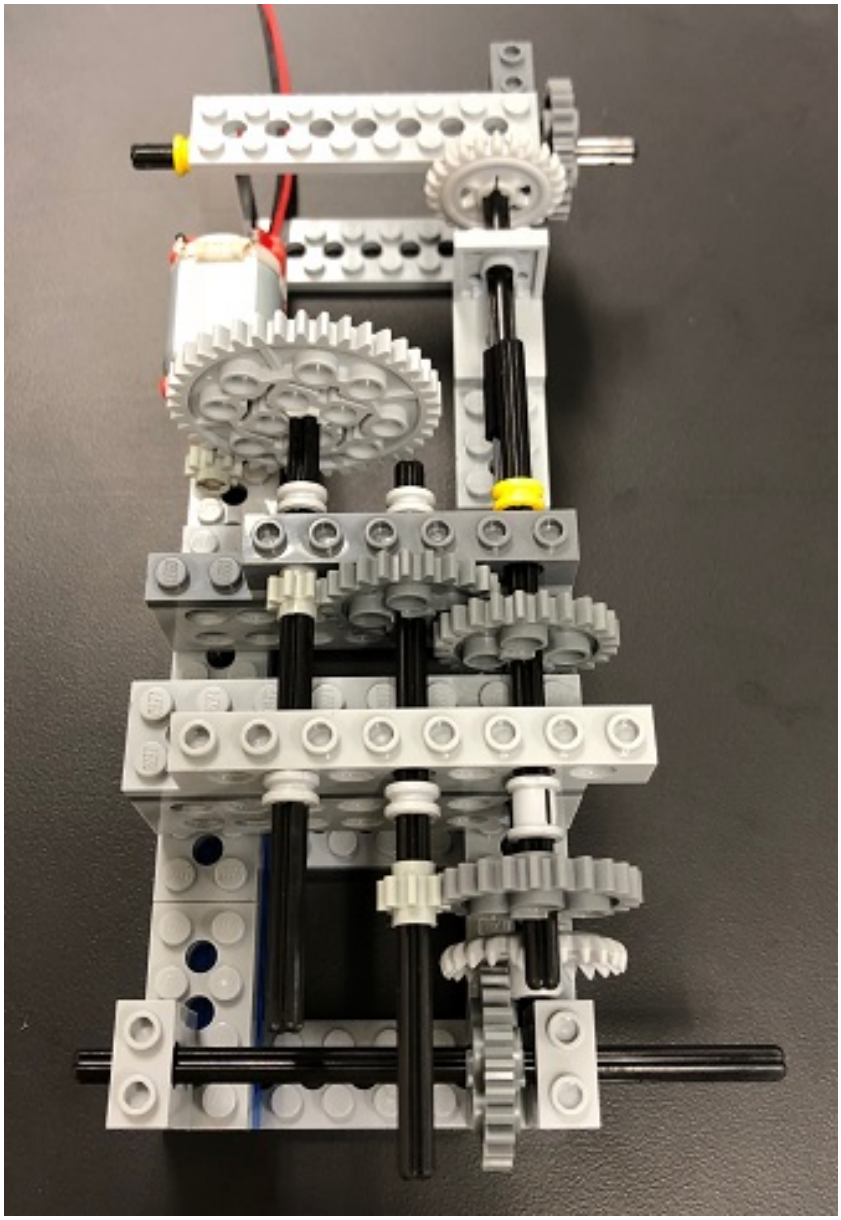

Figure A.3: *Crawler iteration 3.*

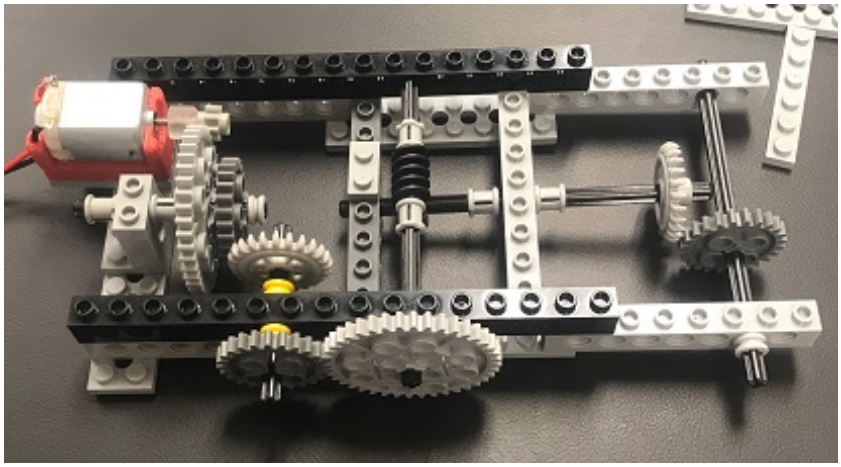

Figure A.4: *Crawler iteration 4.*

A.2 Salamander Retrieval Design Iterations

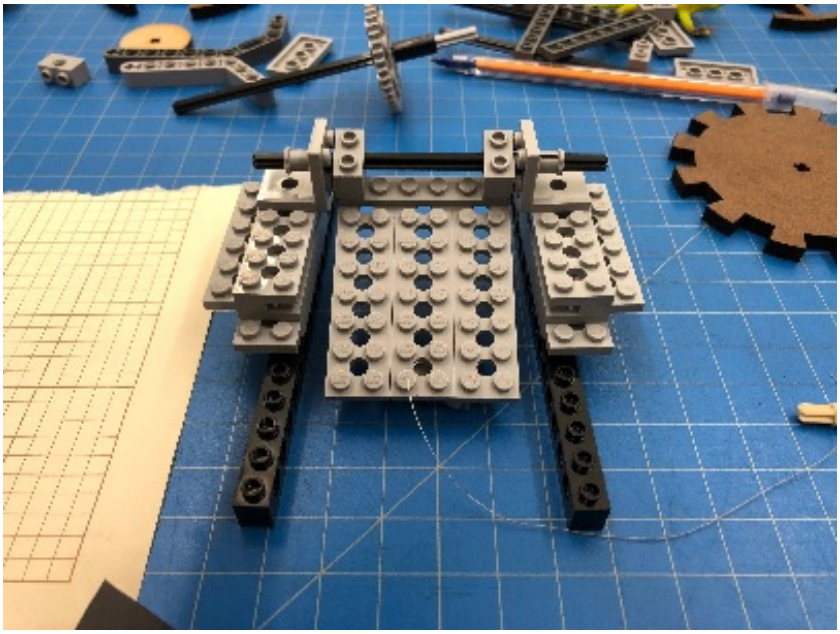

Figure A.5: *Salamander retrieval design iteration 1.*

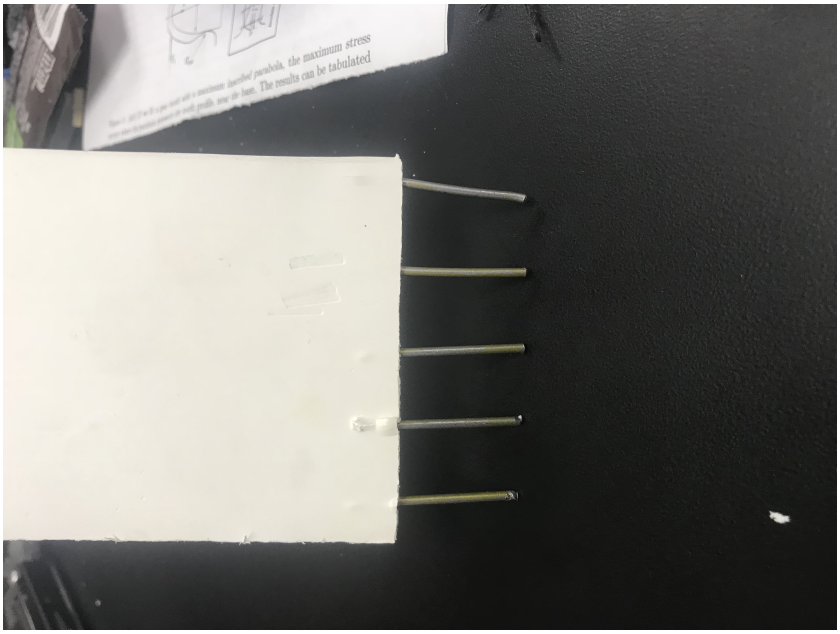

Figure A.6: *Salamander retrieval design iteration 2.*

B Power Flow Analysis

B.1 Variables

Symbol	Value	Units	Definition
V	6	V	Input voltage from power source
I	0.24	A	Input current from power source
I_s		A	Motor stall current
I_{nl}		A	Motor no load current
R	8.91	Ω	Motor resistance
k	4.29×10^{-3}	V/rad/s	Torque constant
T_f	2.54×10^{-4}	Nm	Frictional torque
T_m	1.01×10^{-3}	Nm	Motor torque
T_L	7.54×10^{-4}	Nm	Load torque
F_{roll}		N	Rolling resistance force
F_{out}		N	Propulsion force
F_{pull}	0.44	N	Force required to pull crawler in drag test
ω_L	911	rad/s	Motor load angular velocity
$\omega_{w,f}$	6.85	rad/s	Angular velocity of front wheels
$\omega_{w,b}$	8.21	rad/s	Angular velocity of back wheels
ω_w	7.53	rad/s	Average angular velocity of wheels
g	9.81	m/s^2	Gravitational constant
r_w	0.076	m	Wheel radius
v_x	0.29	m/s	Translational velocity of crawler
m	0.045	kg	Mass required to pull crawler in drag test
GR_f	133		Gear ratio of front wheel axle
GR_b	111		Gear ratio of back wheel axle
P	1.41	W	Power out of source
P_m	0.69	W	Power out of motor
P_t	0.25	W	Power out of transmission
P_w	0.13	W	Power out of wheels
P_R	0.49	W	Power loss due to coil resistance
P_f	0.23	W	Power loss due to frictional torque
$P_{t,l}$	0.43	W	Power loss to transmission
P_r	0.12	W	Power loss due to rolling resistance
P_s	0.12	W	Power loss due to slippage
E_{test}	9.71	J	Energy used in final test
η_m	0.49		Motor efficiency
η_t	0.37		Transmission efficiency
η_w	0.51		Wheel efficiency
η_{net}	0.09		Total efficiency

Table B.1: *Variables used in power flow analysis*

B.2 Diagram Indices

Index	Symbol	Equation	Value
1	P	VI	1.41 W
2	P_R	I^2R	0.49 W
3	P_f	$T_f\omega_L$	0.23
4	P_m	$T - L\omega_L$	0.69
5	$P_{t,l}$	$F_{f,t}\omega_w$	0.43
6	P_t	$T_w\omega_w$	0.25
7	P_r	$T_{roll}\omega_w$	Included in P_w
8	P_s	$(r_w\omega_w - v_x)F_{pull}$	0.12
9	P_w	$F_{out}v_x$	0.13

Table B.2: *Power flow diagram indices*

B.3 Motor Characteristics

V (V)	I_s (A)	R (Ω)
3	0.37	8.11
4	0.47	8.51
5	0.57	8.77
6	0.67	8.96
7	0.73	9.59
8	0.84	9.52

Table B.3: *Stall test data*

V (V)	I_{nl} (A)	ω_{nl} (rad/s)	k (V/rad/s)	T_f (Nm)
0	0	8.11	0	0
3	0.04	8.11	667	1.59×10^{-4}
4	0.05	8.51	877	2.03×10^{-4}
5	0.05	8.77	1090	2.09×10^{-4}
6	0.06	8.96	1283	2.56×10^{-4}
7	0.07	9.59	1421	3.14×10^{-4}
8	0.08	9.52	1524	3.83×10^{-4}

Table B.4: *No load test data*

$$V - IR - k\omega = 0 \tag{B.1}$$

$$kI - T_f = T_L \tag{B.2}$$

$$V - I_s R = 0 \tag{B.3}$$

$$kI_s - T_f = T_s \tag{B.4}$$

$$V - I_{nl} R - k\omega_{nl} = 0 \tag{B.5}$$

$$kI_{nl} - T_f = 0 \tag{B.6}$$

$$P_m = \frac{(kI - T_f)(V - IR)}{k} \tag{B.7}$$

$$\eta_m = \frac{P_m}{P} = \frac{T_L \omega_L}{VI} = \left(\frac{V - IR}{k}\right)\left(\frac{kI - T_f}{VI}\right) \tag{B.8}$$

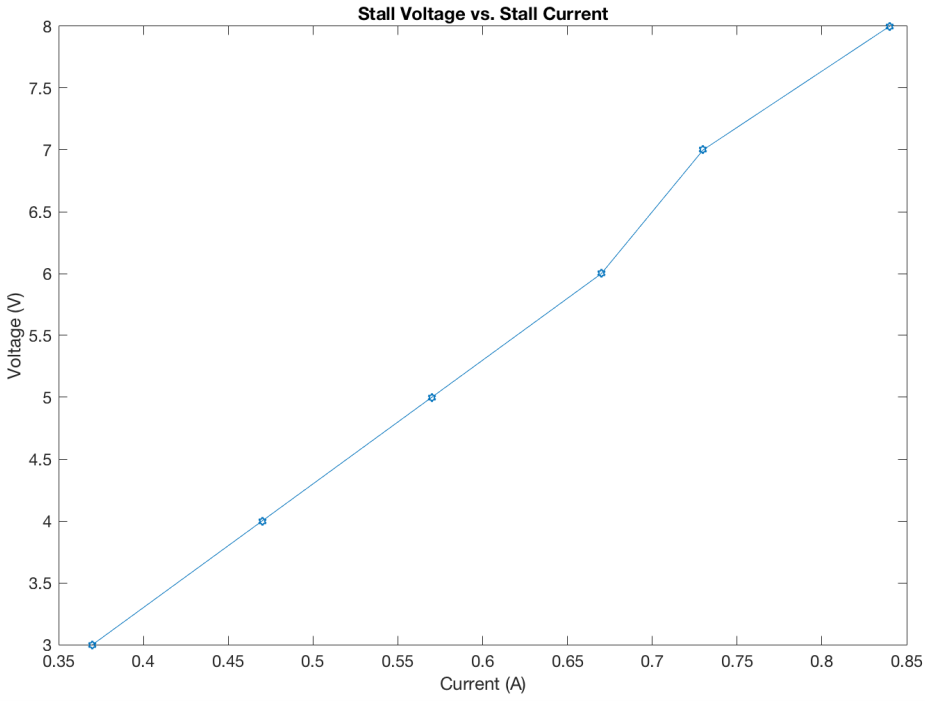

Figure B.1: *Voltage vs. current in stall test*

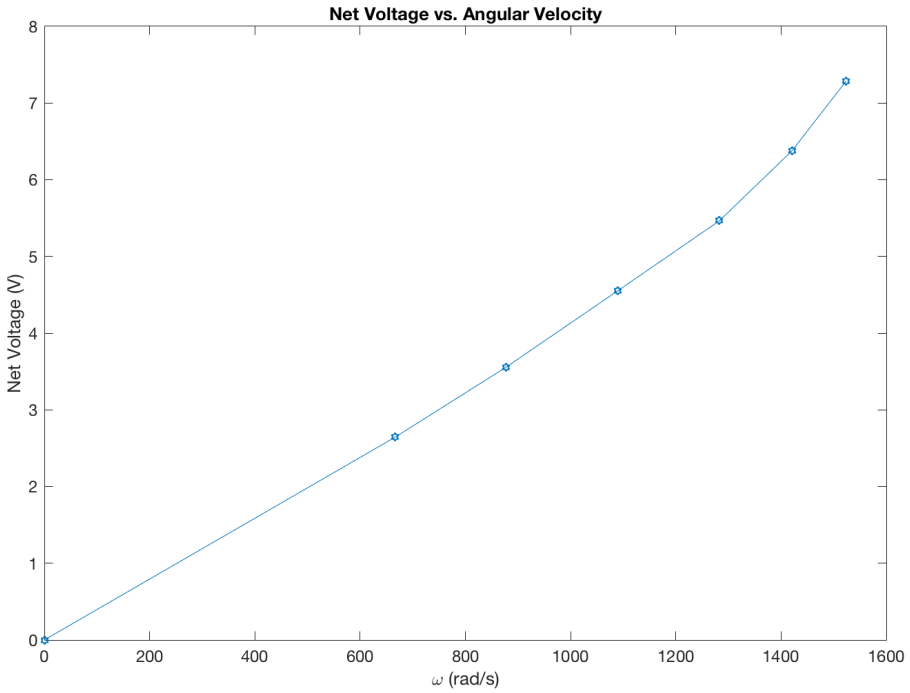

Figure B.2: *Net voltage vs. angular velocity in no load test*

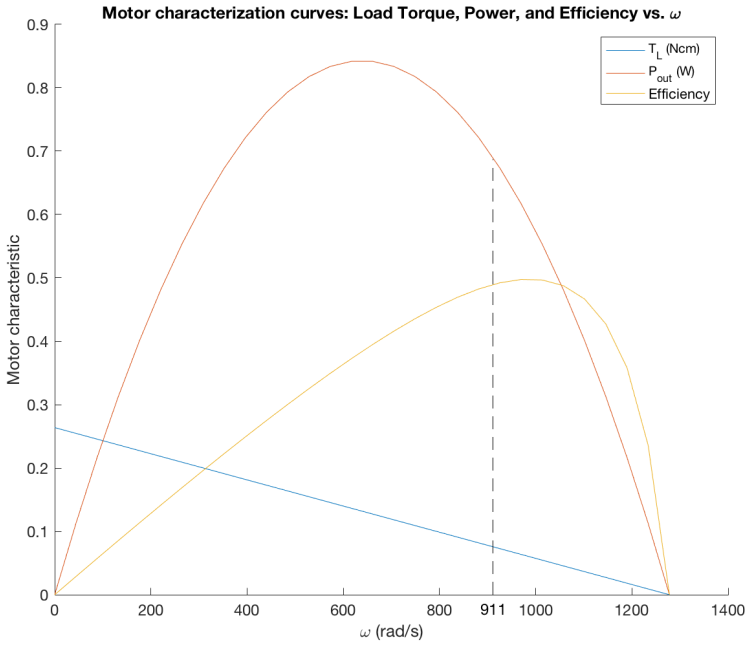

Figure B.3: *Current, power and efficiency for our electric motor. The dotted line marks where on the plot our crawler was operating.*

B.4 Drag Test

m	0.045 kg
F_{pull}	0.44 N

Table B.5: *Results from rolling resistance drag test*

$$F_{pull} = mg \tag{B.9}$$

B.5 Pulley Test

	Front Axle	Rear Axle
GR	133	111
m_i	0.013 kg	0.013 kg
m_{th}	1.729 kg	1.443 kg
m_o	0.262 kg	0.238 kg
η_t	15.15%	16.49%

Table B.6: *Results from transmission pulley test*

$$m_{th} = m_i GR \tag{B.10}$$

$$\eta_t = \frac{m_o}{m_{th}} \tag{B.11}$$

C Gear Strength and Stress Analysis

C.1 Gear Strength Analysis

$$\sigma_n = \sigma'_n C_l C_g C_s K_t K_{ms} K_r; \tag{C.1}$$

$$\sigma_w = \frac{F_t P K_o K_m K_v}{bJ}; \tag{C.2}$$

$$T_g = \eta N_g \omega_L; \tag{C.3}$$

$$F_a = F(cos(\phi)cos(\lambda_w) - \mu sin(\lambda_w)); \tag{C.4}$$

C.2 Gear Strength Constants

Symbol	Value	Notes
K_m	1.6	b $\leq$ 2 and less rigid
K_o	1.5	Moderate shock
Pressure angle	20 (°)	
Q_v	9	Given for Lego gears
b	0.14 (in)	
P	25.4 (teeth/in)	
C_s	0.85	Plastic
C_l	1	Loading type bending
C_g	1	P $\geq$ 5
K_r	0.897	90% reliability
K_t	1	Moderate temperatures
K_{ms}	1.4	Not idler
K_f	0.5	Non-infinite lifetime
K_{ms}	1.4	Not idler
F_t	0.642 (lbf)	
K_v	1.062	
J_{Lewis}	0.657	
η	0.587	
N_g	40 (teeth)	
F	1.22 (N)	
μ	0.1	
ϕ	0.174 (°)	
λ_w	0.144 (°)	

Table C.1: *Constants used to calculate gear stresses*